QUASIELASTIC LIGHT-SCATTERING STUDY ON CHANGES IN SIZES OF NATIVE WHITE MEMBRANES AFTER ADDITION OF RETINAL

JEFFREY MARQUE,* AKIRA IKEGAMI,* KENJI KUBOTA,‡ YASUNORI TOMINAGA,‡ AND SATORU FUJIME§

**The Institute of Physical and Chemical Research, 2-1 Hirosawa, Wako, Saitama 351-01, Japan;*
‡*Department of Physics, Faculty of Science, Ochanomizu University, Bunkyo-ku, Tokyo 112, Japan;*
and §*Mitsubishi-Kasei Institute of Life Sciences, Machida, Tokyo 194, Japan*

ABSTRACT Aqueous suspensions of native white membranes from *Halobacterium halobium*, strain JW2N, have been studied by quasielastic light scattering. The intensity autocorrelation functions of polarized scattered light from suspensions of white membranes themselves and of white membranes after reconstitution with retinal were measured at various K^2, K being the magnitude of the scattering vector. The first cumulant or the average decay rate of the correlation function was obtained by a cumulant expansion method. The first cumulant for the white membranes increased after retinal was added to the suspension. The first cumulants obtained before and after the addition of retinal were almost independent of pH in the range 7 to 11, and of temperature in the range 15° to 40°C after T/η scaling, η being the solvent viscosity. This suggests that photocycling in reconstituted membranes, induced by the probe laser-beam, did not cause any detectable change in spectra, and that the membrane flexibility, if present, was independent of the above conditions, so that the spectral changes after the addition of retinal could be attributed mostly to the changes in the sizes of the membranes. A theoretical formulation for the first cumulant for a rigid disk-like scatterer (Fujime, S. and K. Kubota, 1985, *Biophys. Chem.*,23:1–13.) was applied to the analysis of the spectra. The results suggest that the radii of the membrane patches decreased by several percent after the addition of retinal.

INTRODUCTION

Purple membrane is the light-driven proton pump found in the cell membrane of *Halobacterium halobium*. We summarize here some results reported in the literature, which have direct relevance to our study. For further information about purple membrane or its sole constituent protein, bacteriorhodopsin, we refer the reader to any of several review articles (Henderson, 1977; Stoeckenius et al., 1979; Stoeckenius and Bogomolni, 1982).

One of the striking features of purple membrane that distinguishes it from many other biomembranes, and that has made it such an attractive subject for study, is its crystalline structure. In native purple membrane, bacteriorhodopsin forms a two-dimensional hexagonal lattice in the plane of the membrane (Stoeckenius et al., 1979). We know that each unit cell of the crystal contains a trimer of proteins, but the functional significance of the trimer is subject of controversy. Cooperativity of photocycling among adjacent bacteriorhodopsin molecules has been reported (Korenstein and Hess, 1982), and some investigators have also compared photocycle kinetics and stoichiometry between the monomeric form and the crystalline (trimeric) form of the protein (Dencher and Heyn, 1979; Dencher et al., 1983). Although photocycling activity and proton pumping have been observed in monomers, the efficiency of light-adaption in monomers is less than in the crystalline form (Dencher et al., 1983). The organization of bacteriorhodopsin into a lattice, and the interaction leading to that organization, therefore, seem physiologically important.

Several workers have investigated mechanical and thermodynamic properties of the purple membrane lattice (Jackson and Sturtevant, 1978; Jippo et al., 1983; Marque et al., 1984; Tristram-Nagle et al., 1985). The apparent specific volume, expansivity and compressibilities (adiabatic and isothermal) that have been measured have the values near to what would be expected based on the mass fractions of lipid and protein molecules in the membrane and on previously measured values of those thermodynamic quantities for lipid and proteins. However, the value for the specific heat at constant pressure is anomalous (Marque et al. 1984).

Native membranes formed by bacterio-opsin are far less well-characterized thermodynamically and structurally than purple membrane. In addition, there are some apparent discrepancies reported in the literature that may be

Jeffrey Marque's present address is School of Applied and Engineering Physics, Cornell University, Clark Hall, Ithaca, New York 14853.
Correspondence should be addressed to Kenji Kubota.

implicitly important for understanding protein-protein interactions in the purple membrane and, perhaps, the physiological significance of the lattice. Mukohata et al. (1981) claim that freeze fracture electron micrographs show the same crystalline ordering of bacterio-opsin in white membranes as bacteriorhodopsin in purple membranes. Sumper et al. (1976) believe that crystallization occurs only after the addition of retinal to membranes containing bacterio-opsin. Mukohata et al. (1981) and Stoeckenius et al.(1979) reported the same locations for white and purple membranes, respectively, in a sucrose gradient (1.18 g/mL), but Sumper et al. (1976) found a different buoyant density in purple membranes compared with membranes with bacterio-opsin. In addition, Schoeningh found a different lipid-to-protein ratio in purple membranes compared with white membranes (unpublished results mentioned in Oesterhelt, 1982). Hwang et al. (1981) reported that brown membrane, i.e., "purple" membrane grown in the presence of nicotine, an inhibitor of retinal synthesis, has no periodicity in the plane of the membrane, but that crystallization occurs after the membrane is rendered purple by reconstitution with retinal. We do not know if there are fundamental differences between "white membranes" and "brown membranes," but we shall in this paper assume that there are not. We refer to our sample as white membranes, even though concentrated suspensions of the membrane are of a light brown color. Their absorption spectrum exhibits a peak at 410–412 nm. They had no periodic structure prior to the addition of retinal (Furuno and Marque, unpublished x-ray results); however the addition of retinal caused crystallization of proteins in the membrane into a form whose x-ray scattering pattern showed the same lattice constants as native purple membranes. It is possible, but perhaps unlikely, that bacterio-opsin crystallizes in some native membranes but not in others.

Quasielastic light scattering has already been used to study the spectrum from suspensions of purple membranes (Kubota et al., 1985). General background information about quasielastic light scattering is found in standard textbooks (Berne and Pecora, 1975; Chu, 1974). In the present study, we use quasielastic light scattering to study the changes in the hydrodynamic properties of white membranes that occur when retinal is added to the membrane suspension. As will be seen in the remainder of this paper, reconstitution of white membranes causes distinct changes in hydrodynamic properties of the membrane.

MATERIALS AND METHODS

White Membrane Production

Halobacterium halobium, strain JW2N, was the kind gift of Professor Koji Nakanishi (Department of Chemistry, Columbia University, New York). The bacteria were raised on the synthetic medium described by Onishi et al. (1965), with slight modifications and one addition: We used only L amino acids, and where applicable therefore halved the quantities of the amino acids indicated in Onishi et al.; in addition, we added, for each liter of culture, 20 g of DL malic acid, disodium salt. After final mixing of the medium, the pH was adjusted to 6.2 with KOH or NaOH. We used synthetic media because we obtained consistently higher yields than with media based on peptone. The bacteria were harvested and white membranes isolated and purified according to Oesterhelt (1982). However, in contrast to the description by Oesterhelt, we found white membranes in significant amounts throughout >50% of the length of the sucrose gradient, with the lightest fraction being found at the top of a very prominent brown band. We used polyacrylamide gel electrophoresis in the presence of sodium dodecyl sulfate (SDS) to detect protein impurities in our white membrane samples. We invariably found protein impurities that were of higher and lower molecular weight than bacterio-opsin, and no amount of washing or sonication gave such pure samples as we obtained with purple membranes. However, the estimated intensities of the impurity bands compared with the bacterio-opsin band (the latter band determined by using both purple membranes and papain-treated purple membranes for calibration bands) suggested that at least 90% of the protein in our preparation was bacterio-opsin.

Preparation of Scattering Samples

An unbuffered aqueous suspension of white membranes (later referred to as suspension X) was prepared with an estimated bacterio-opsin concentration of 15 μM, and 3 ml of the suspension were titrated against 5 μl aliquots of 1 mM all-*trans* retinal in methanol, while the absorbance of the sample at 560 nm was monitored in a spectrophotometer. Saturation of the opsin with retinal was indicated when the addition of an aliquot of retinal solution yielded no further increase in the absorbance. The difference in the absorbance at 560 nm of the retinal-saturated suspension compared with the retinal-free suspension was then multiplied by 16 μM to obtain an estimate of the bacteriorhodopsin concentration, hereafter referred to as C(bR), in the reconstituted suspension. Next, partially reconstituted suspensions of white membranes were prepared from suspension X by the same procedure as just described above except that, as a precaution, reconstitution was done in a dark room. In the partially reconstituted suspensions, hereafter referred to as samples *A*, *B*, and *C*, the amounts of retinal added were such that the final concentrations of retinal (bound plus unbound) were, respectively, 1.0C(bR), 0.47C(bR), and zero. With the exception of the very small protein concentration differences due to different amounts of retinal-methanol added, the above three suspensions were identical except for the amounts of retinal added to them.

For light scattering measurements, an aliquot of one of the final suspensions described above was mixed with water and one of several 50-mM buffer stock solutions (pH 7: HEPES, pH 10 and 11; bicarbonate) so that the final buffer concentration was 8 mM and the final protein concentration, equal to within <3% in the three suspensions, was equal to ~1 μM. We were able to confirm the approximate protein concentration by comparing the scattering intensity with that obtained from purple membrane suspensions of 1-μM bacteriorhodopsin. The suspensions were filtered through a membrane filter (Nucleopore Corp., Pleasanton, CA) with 0.6-μm pore size, directly into a 10-mm o.d. polished cylindrical cell that had been previously thoroughly washed and rinsed.

Light Scattering Apparatus

The light scattering measurements were carried out with a homemade spectrometer and a 252-channel real-time digital correlator. The details of this system are described elsewhere (Kubota et al., 1984). We used an argon ion laser (model GLG-3200; Nippon Electric Company, Tokyo) operating at 488.0 nm, with a radiant power of <5 mW at the sample cell. The temperature was regulated to within 0.02°C in all measurements.

Data Analysis

The homodyne intensity correlation function, $G^2(\tau)$, is related to the normalized field correlation function, $g^1(\tau)$, by

$$G^2(\tau) = A(1 + \beta|g^1(\tau)|^2), \quad (1)$$

where A is the baseline, β is a machine constant, and τ is the delay time. For a monodisperse suspension of spheres, $g^1(\tau)$ has the simple form of $g^1(\tau) = \exp(-\Gamma\tau)$, where $\Gamma = DK^2$, D is the translational diffusion coefficient, and K is the magnitude of the scattering vector. However, if, as in our system of membrane patches, the scatterers are polydisperse and have various motions other than translation, then $g^1(\tau)$ is expressed as a sum of exponential decays. Another expression for $g^1(\tau)$, the cumulant expansion (Koppel, 1972), is useful for describing these contributions,

$$g^1(\tau) = \exp(-\bar{\Gamma}\tau) \times [1 + \mu_2\tau^2/2! - \mu_3\tau^3/3! + \ldots], \quad (2)$$

where $\bar{\Gamma}$ is the average decay rate or the first cumulant and μ_i is the ith moment around $\bar{\Gamma}$ of $G(\Gamma)$, the decay rate distribution function. In particular, $\mu_2/\bar{\Gamma}^2$ is the normalized dispersion. Due to the polydispersity of our white membrane suspensions, we choose to use $\bar{\Gamma}$ as the most characteristic measure of the correlation function. A theoretical expression for the first cumulant for rigid disk-like scatterers with radius R has been given (Fujime and Kubota, 1985),

$$\bar{\Gamma}/K^2 = D_0 + (R^2/4)\Theta g_1(KR) + (D_3 - D_1)[g_2(KR) - 1/3], \quad (3)$$

where D_0, D_1, D_3, and Θ are, respectively, the average translational diffusion coefficient, the translational diffusion coefficients parallel and perpendicular to the disk plane, and the rotational diffusion coefficient of the disk. $g_1(KR)$ and $g_2(KR)$ are functions depending only on KR, and their numerical values are tabulated elsewhere (Kubota et al., 1985). In the limit of $KR = 0$, we have $g_1 = 0$ and $g_2 = 1/3$, so that $\bar{\Gamma}/K^2$ in the small K limit gives the average translational diffusion coefficient D_0. At large K^2, $\bar{\Gamma}/K^2$ shows contributions from other motions.

The values of the diffusion coefficients of an extremely oblate ellipsoid of revolution (or a thin disk) with radius R are given by Perrin's formulas (Perrin, 1934):

$$D_0 = k_B T/12\eta R$$
$$D_1 = 3k_B T/32\eta R$$
$$D_3 = k_B T/16\eta R$$
$$\Theta = 3k_B T/32\eta R^3, \quad (4)$$

where η is the viscosity of the medium, k_B is the Boltzmann constant and T is the absolute temperature.

RESULTS AND DISCUSSION

Fig. 1 shows $\bar{\Gamma}/K^2$ vs. K^2 obtained from the third-order cumulant fit to the correlation functions from samples A, B, and C at 25°C and 8-mM HEPES buffer (pH 7). The concentrations of membranes were the same in these three samples and were sufficiently dilute so that, in the absence of membrane aggregation, intermembranal interactions did not contribute to the correlation functions. The overall behavior of these three curves is quite similar to that of purple membranes (Kubota et al., 1985). Sample C seems to exhibit slight wiggling of $\bar{\Gamma}/K^2$ in the intermediate range of K^2, a characteristic feature of disk-like scatterers. The wiggling is attenuated by the polydispersity of the sample, and even disappears in the spectra for samples A and B. The polydispersity is confirmed by the fact that the typical value of $\mu_2/\bar{\Gamma}^2$ was ~0.2. Unambiguous features of Fig. 1 are that (a) the magnitudes of $\bar{\Gamma}/K^2$ for white membranes with added retinal are larger for all scattering angles than

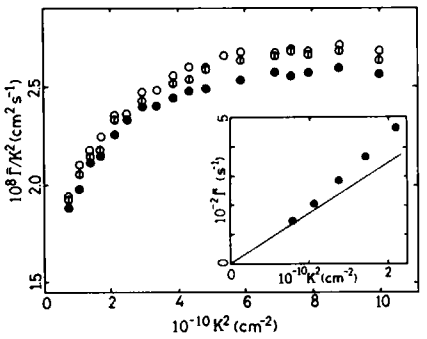

FIGURE 1 $\bar{\Gamma}/K^2$ vs. K^2 for samples A (○), B (◐), and C (●) at 25°C and 8 mM HEPES buffer (pH 7.0). The relative amounts of added retinal were, respectively, 1.0, 0.47, and 0. The *inset* shows the initial portion of $\bar{\Gamma}$ vs. K^2 for sample C, where the straight line has the slope of 1.75×10^{-8}cm^2/s.

those for retinal-free membranes, and (b) the increase in the $\bar{\Gamma}/K^2$ values varies directly with the amount of retinal that was added. At the small K^2, we see no drastic changes in the $\bar{\Gamma}/K^2$ values, implying that the binding of retinal to the membranes occurs without detectable aggregation and/or disintegration of the membranes. As a control blank, we added comparable aliquots of methanol (the retinal solvent) to suspensions of white membranes, and detected no changes in the spectra.

An increase in $\bar{\Gamma}/K^2$ was observed every time we added retinal until retinal was present in excess, at which point the increase ceased. We conclude that the change in the spectrum is associated with the binding of retinal to bacterio-opsin. We expect that the spectral changes shown in Fig. 1 are characterized by the same membrane properties (e.g., average sizes, size distribution, noncircular shape, and internal motions) as those included in the analysis of dynamic light-scattering spectra from suspensions of purple membranes (Kubota et al., 1985).

An extrapolation of the $\bar{\Gamma}/K^2$ values to $K = 0$ for sample C gives an average translational diffusion coefficient of $(1.75 \pm 0.05) \times 10^{-8}$ cm^2/s. This value and the Perrin's formula for D_0 in Eq. 4 give a z-average mean radius of 220 nm (or strictly speaking, $\langle 1/R \rangle_z^o = (220\text{ nm})^{-1}$; see below for the definition of $\langle 1/R \rangle_z^o$). The above extrapolation of $\bar{\Gamma}/K^2$ values to $K = 0$, or the determination of the initial slope in $\bar{\Gamma}$ vs. K^2 (see *inset* in Fig. 1), was not unequivocal because of the lack of data at very low K^2. Then, the estimated value of the average radius was examined to be consistent with the first peak position in $K^2I(KR)$ vs. K^2, where $K^2I(KR)$ is the K^2-weighted static scattering intensity (Kubota et al., 1985). Samples A and B have almost the same extrapolated values of $\bar{\Gamma}/K^2$ at $K = 0$.

In thinking about explanations for the larger $\bar{\Gamma}/K^2$ values in samples A and B than in sample C, we examined the possibility that the local temperature of reconstituted membranes (which are purple) may increase due to the absorption of the incident beam. This was done by measuring correlation functions with various powers of the incident beam and with white actintic light. $\bar{\Gamma}/K^2$ vs. K^2

showed no beam-power dependence. We conclude that the increase in $\bar{\Gamma}/K^2$ after reconstitution is not due to heating.

X-ray data indicate that crystallization of opsin occurs after addition of retinal to our white membrane suspensions (Furuno and Marque, unpublished results). In general, such phase changes from a nonordered to an ordered state may be accompanied by an increase in elastic moduli and decrease in flexibility. Since a theory for quasielastic light scattering from two-dimensional flexion motions does not exist, we draw on analogy from the theory of flexible rods (Fujime and Maeda, 1985, see also Appendix), where decreases in flexibility are accompanied by decreases in $\bar{\Gamma}/K^2$: Analogy suggests that in our membrane system, the observed increase in $\bar{\Gamma}/K^2$ is not due to a flexibility decrease that may occur during crystallization of opsin.

Any motion of individual photocycling proteins can not be "seen" by a probe of visible light because the amplitudes of motions of proteins are much smaller than the inverse length of the scattering vector, $1/K$. However, if motions (and/or states) of proteins could induce appreciable changes in the membrane flexibility, we might expect to detect the effect of photocycling on the $\bar{\Gamma}/K^2$ values for large K. Although only a small fraction of the bacteriorhodopsin molecules are expected to be excited by the probe beam at the power and wavelength in our experiments, we now examine the question of whether photocycle intermediates might be responsible for the differences in the spectra shown in Fig. 1. Fig. 2*a* shows the pH dependence of $\bar{\Gamma}/K^2$ values for samples *A* and *C*, where a very slight pH dependence in the $\bar{\Gamma}/K^2$ values is observed for reconstituted membranes (sample *A*). Fig. 2*b* shows the temperature dependence of $\bar{\Gamma}/K^2$ values for samples *A* and *C*, respectively. The data at 15° and 40° are corrected to 25°C by T/η scaling. This figure shows that the scaled data are temperature independent. (The same temperature independence has been observed in purple membrane suspensions (Kubota et al. 1985). The results of these pH and temperature experiments suggest that photocycling in reconstituted membranes, itself highly pH and temperature dependent, does not cause any detectable change in spectra when induced by the probe laser beam. However, it should be noted that these results do not necessarily exclude the possibility that membrane flexion modes contribute to $\bar{\Gamma}/K^2$ at large K^2. They suggest only that the membrane flexibility, if present, is very insensitive to pH and the temperature of the suspension (see Appendix). Unfortunately, we have no way, at the moment, of estimating the size of flexion mode contributions to $\bar{\Gamma}/K^2$. In what follows, therefore, we assume that the observed $\bar{\Gamma}/K^2$ in Fig. 1 are due only to the translational and rotational motions of the membranes.

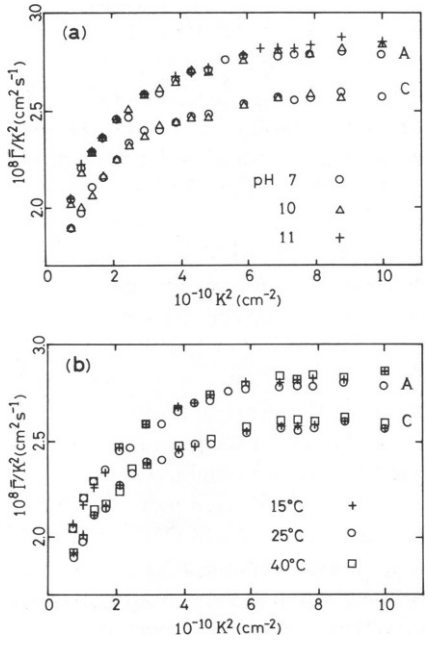

FIGURE 2 $\bar{\Gamma}/K^2$ vs. K^2 for samples *A* and *C* under various conditions. (*a*) At 25°C and different pHs; (*b*) at pH 7.0 and different temperatures after T/η correction to 25°C. To avoid the cluttering, $\bar{\Gamma}/K^2$ values for sample *A* are shifted upward by 0.1 units in both (*a*) and (*b*).

We study the increase in the $\bar{\Gamma}/K^2$ after reconstitution by examining the ratios of the first cumulants for sample *A* as compared with sample *C*, and for sample *B* as compared with *C*. The ratios are plotted in Fig. 3. The ratios shown are more sensitive indicators of the changes of membrane properties than the absolute values of the first cumulants. Thus, Fig. 3 gives information about the increase in the first cumulant when protein crystallizes. The ratio seems to increase slightly with K^2 and does not go to unity at $K = 0$. We can, a priori, invoke size change and/or size distribution change as the underlying reasons for the observed nonunity ratios shown in Fig. 3. As in the earlier purple membrane work (Kubota et al., 1985), we characterize the polydispersity with the Schulz-Zimm distribution function,

$$W(R)\mathrm{d}R = [1/\Gamma(m+1)]\,(m+1)^{m+1}\,(R/\bar{R})^m \exp[-(m+1)R/\bar{R}]\mathrm{d}(R/\bar{R}), \quad (5)$$

where $W(R)$ is the number fraction of disks having radii in a range R and $R + \mathrm{d}R$, $\bar{R}$ is the number-weighted average radius, m is the measure of polydispersity, and $\Gamma(m+1) = m\Gamma(m)$ is the Gamma function, which equals $m!$ for integers. From Eq. 3 and the Perrin's formula for D_0 in Eq. 4, we have

$$\langle D_0\rangle_z^o = \bar{\Gamma}/K^2|_{K\to 0} = (k_BT/12\eta)\,\langle 1/R\rangle_z^o, \quad (6)$$

where $\langle\ldots\rangle_z$, which was previously denoted as $\langle\ldots\rangle_h$ (Kubota et al., 1985), stands for the light-scattering z-average and the superscript o stands for the average at $K = 0$; $\langle f(R)\rangle_z^o = \int f(R)R^pW(R)\mathrm{d}R / \int R^pW(R)\mathrm{d}R$ with $p = 4$ for a disk. As shown previously, we have for $W(R)$ in Eq. 5

$$\langle 1/R\rangle_z^o = [(m+1)/(m+4)](1/\bar{R}). \quad (7)$$

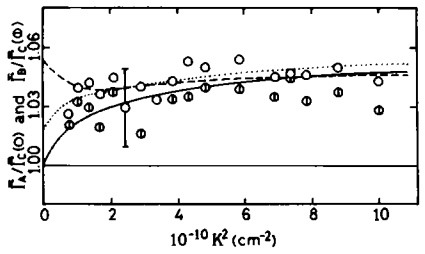

FIGURE 3 $\bar{\Gamma}_A/\bar{\Gamma}_C$ (O) and $\bar{\Gamma}_B/\bar{\Gamma}_C$ (O) vs. $K^2 \cdot \bar{\Gamma}_X$ (X = A, B, or C) denotes the first cumulant for sample X. The dashed curve stands for the calculated ratio $\bar{\Gamma}(209, 7)/\bar{\Gamma}(220, 7)$, the dotted curve for $\bar{\Gamma}(216, 6)/\bar{\Gamma}(220, 7)$, and the solid curve for $\bar{\Gamma}(220, 5.5)/\bar{\Gamma}(220, 7)$, where $\bar{\Gamma}(R, m)$ denotes the calculated first cumulant for $\langle 1/R \rangle_z^o = (R \text{ nm})^{-1}$ and the polydispersity parameter m. For details, see text.

Assuming that the membranes are disks, the best distribution parameter to describe sample C with $\langle 1/R \rangle_z^o = (220 \text{ nm})^{-1}$ is $m = 7$, or $\bar{R} = 160$ nm. The calculated dependence of $\bar{\Gamma}/K^2$ on K^2 is shown in Fig. 4. (Details of the algorithm for calculation, and dependence on K^2, of $\langle D_0 \rangle_z$, $\langle (R^2/4)\Theta g_1(KR) \rangle_z$ and $\langle (D_3 - D_1)\,[g_2(KR) - 1/3] \rangle_z$ (Eq. 3) for different values of the polydispersity parameter m are found in the Appendix of Kubota et al., 1985.) At $K^2 < 1.5 \times 10^{10}$ cm^{-2}, a discrepancy between calculated and measured curves is observed; this can be attributed partly to the effect of noncircular shape of white membranes (as discussed previously (Kubota et al., 1985)), partly to slight heterodyning at the lowest K^2, and partly to at least one more source discussed in the Appendix of this paper. If we now find the best-fit parameters for sample A by imposing no constraint on $\langle 1/R \rangle_z^o$ or m, we obtain $\langle 1/R \rangle_z^o = (216 \text{ nm})^{-1}$ and $m = 6$, or $\bar{R} = 151$ nm. If we use the constraint $m = 7$, the same as that for white membranes (sample C), then we obtain $\langle 1/R \rangle_z^o = (209 \text{ nm})^{-1}$, or $\bar{R} = 152$ nm. Since it is not clear whether or not the ratios in Fig. 3 go to unity at $K = 0$, we also examine the case of $\langle 1/R \rangle_z^o = (220 \text{ nm})^{-1}$ for both samples A and C. Then, we obtain the best-fit parameter of $m = 5.5$, or $\bar{R} = 150$ nm, for sample A. The calculated $\bar{\Gamma}/K^2$ vs. K^2 relationships for sample A are also shown in Fig. 4, and discrepancies at low K^2 are due to the same reasons as those for white membranes (sample C). The ratios of the first cumulants for these cases are shown in Fig. 3, where it is seen that the model cases considered are all consistent with the observed ratios.

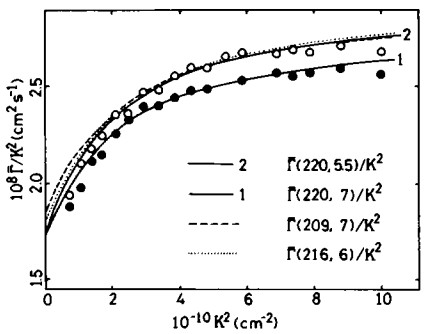

FIGURE 4 Comparison of calculated $\bar{\Gamma}/K^2$ vs. K^2 relationships with the measured ones (O) for sample A and (●) for sample C. The definition of $\bar{\Gamma}(R, m)$ is the same as that in Fig. 3.

For a given value of $\langle 1/R \rangle_z^o$, $W(R)$ for $m = 5.5$ becomes larger than $W(R)$ for $m = 7$ beyond a certain but large R^* value. However, this does not affect our analysis, because the number of membranes with radii $R \geq R^*$ is only a very small fraction of the total. We conclude that the mean radius $\bar{R}$ of the membranes decreases by 5–6% after retinal is added to white membrane suspensions, or after the protein crystallizes. Such an interpretation is conditional upon considerations in the Appendix.

A decrease in radius by 3% corresponds to an increase in the mass density by 6% provided that the thickness is unchanged. Such a large change in density might affect various physical properties. The sound velocity, for example, through suspensions of white membranes increases after retinal is added and the membranes have become purple (Mitaku et al., unpublished data). The product of the suspension density and the suspension adiabatic compressibility thus decreases. Our result may be helpful in interpreting this, and perhaps other, observations concerning crystallization of white membranes.

APPENDIX

Analogy to the theory of semiflexible rods (Maeda and Fujime, 1984) gives the following expression for semiflexible disks (see Eq. 3).

$$\bar{\Gamma}/K^2 = D_0 + (R^2/4)\Theta g_1(KR) + (D_3 - D_1)\,[g_2(KR) - 1/3] + g_3(KR, \gamma R),$$

where γR is the flexibility parameter and $g_3(KR, \gamma R)$ (≥ 0) stands for contributions from membrane flexion modes. When $\gamma R \neq 0$, $g_3(KR, \gamma R)$ increases with K. When the elastic modulus ϵ of the membrane flexion is proportional to $k_BT/(\gamma R)$, and when γR is independent of solvent conditions such as pH values and temperature, $g_3(KR, \gamma R)$ scales with T/η (Fujime and Maeda, 1982).

In the text, we assumed $g_3(KR, \gamma R) = 0$. But, if, in fact, $g_3(KR, \gamma R) \neq 0$, the size of contributions to $\bar{\Gamma}/K^2$ from translational and rotational modes is smaller than the observed $\bar{\Gamma}/K^2$ at any K ($\neq 0$), especially at large K, and the true polydispersity parameter m might be larger than that estimated in the text (where we assumed $g_3(KR, \gamma R) = 0$). For example, consider the solid lines 1 and 2 in Fig. 4. Discrepancies at low K between calculated and observed $\bar{\Gamma}/K^2$ values in Fig. 4 may be partly due to $g_3(KR, \gamma R) \neq 0$. Since a smaller m gives a smaller $\bar{R}$ for a given $\langle 1/R \rangle_z^o$, the decrease in $\bar{R}$ given in the text is an upper bound. On the other hand, it is expected that the flexibility parameter γR, and hence the size of $g_3(KR, \gamma R)$, will become smaller on crystallization of the protein. In this sense, the estimated size of shrinkage may not necessarily be its upper bound.

If a precise extrapolation of $\bar{\Gamma}/K^2$ to $K = 0$ were possible, a determination of the size of shrinkage would be very much straightforward. For a large scatterers, however, this is not easy when a conventional spectrometer is used. So we adopted a rather indirect procedure in the text. We conclude that, although shrinkage is almost certainly indicated by our data, our lack of information about $\bar{\Gamma}/K^2$ at sufficiently low K^2 and/or about $g_3(KR, \gamma R)$ prevents us from making a precise description of the shrinkage.

We thank Mr. J. Otomo for assistance in production of the membranes and for many helpful discussions. We express our thanks to Professor Koji Nakanishi, from Columbia University in New York City, for providing the bacterial culture used in this study.

This work was partly supported by the following grants; a grant (National Science Foundation INT 8313642) from the U.S. National Science Foundation (U.S.-Japan Program in Photoconversion and Photosynthesis), a research grant for solar energy conversion and photosynthesis from the Agency of Science and Technology of Japan, special coordination funds for the promotion of science and technology from the Agency of Science and Technology of Japan, and the Grant-in-Aid from the Ministry of Education, Science and Culture of Japan.

Received for publication 16 October 1985.

REFERENCES

Berne, B., and R. Pecora. 1975. Dynamic Light Scattering. Interscience, New York. 1–376.

Chu, B. 1974. Laser Light Scattering. Academic Press, New York. 1–317.

Dencher, N. A. 1983. The five retinal-protein pigments of halobacteria: bacteriorhodopsin, halorhodopsin, P565, P370 and slow-cycling rhodopsin. *Photochem. Photobiol.* 38:753–767.

Dencher, N. A., and M. P. Heyn. 1979. Bacteriorhodopsin monomers pump protons. *FEBS (Fed. Eur. Biochem. Soc.) Lett.*108:307–310.

Dencher, N. A., K.-D. Kohl, and M. P. Heyn. 1983. Photochemical cycle and light-dark adaptation of monomeric and aggregated bacteriorhodopsin in various lipid environments. *Biochemistry.*22:1323–1334.

Fujime, S., and T. Maeda. 1982. A note on T/η scaling of dynamic light-scattering spectrum. *Biophys. J.*38:213.

Fujime, S., and T. Maeda. 1985. Spectrum of light quasielastically scattered from dilute solutions of very long and slightly bendable rods. Effect of hydrodynamic interactions. *Macromolecules.*18:191–195.

Fujime, S., and K. Kubota. 1985. Dynamic light scattering from dilute suspensions of thin discs and thin rods as limiting forms of cylinder, ellipsoid and ellipsoidal shell of revolution. *Biophys. Chem.* 23:1–13.

Henderson, R. 1977. The purple membrane from *halobacterium halobium. Annu. Rev. Biophys. Bioeng.* 6:87–109.

Hwang, S.-B., T.-W. Tseng, and W. Stoeckenius. 1981. Spontaneous aggregation of bacteriorhodopsin in brown membrane. *Photochem. Photobiol.* 33:419–427.

Jackson, M. B., and J. M. Sturtevant. 1978. Phase transition of purple membranes of *halobacterium. Biochemistry.*17:911–915.

Jippo, T., R. Kataoka, S. Mitaku, and A. Ikegami. 1983. Critical slowing down in lipid bilayer membrane studied by a differential ultrasonic resonator. *Jpn. J. Appl. Phys.* 23(Suppl. 23–1):63–65.

Koppel, D. E. 1972. Analysis of macromolecule polydispersity in intensity correlation spectroscopy: the method of cumulants. *J. Chem. Phys.* 57:4814–4820.

Korenstein, R., and B. Hess. 1982. Cooperativity of photocycle in purple membrane. *Methods Enzymol.* 88:193–201.

Kubota, K., H. Urabe, Y. Tominaga, and S. Fujime. 1984. Spectrum of light quasielastically scattered from suspensions of tobacco mosaic virus. Experimental study on anisotropy in translational diffusion. *Macromolecules.* 17:2096–2104.

Kubota, K., Y. Tominaga, S. Fujime, J. Otomo, and A. Ikegami. 1985. Dynamic light scattering study of suspensions of purple membrane. *Biophys. Chem.* 23:15–29.

Maeda, T., and S. Fujime. 1984. Spectrum of light quasielastically scattered from solutions of semiflexible filaments at dilute and semidilute regimes. *Macromolecules.* 17:2381–2391.

Marque, J., L. Eisenstein, E. Gratton, J. M. Sturtevant, and C. J. Hardy. 1984. Thermodynamic properties of purple membrane. *Biophys. J.* 46:567–572.

Mukohata, Y., Y. Sugiyama, Y. Kaji, J. Usukura, and E. Yamada. 1981. The white membrane of crystalline bacterioopsin in *halobacterium halobium* strain R_1mW and its conversion into purple membrane by exogenous retinal. *Photochem. Photobiol.* 33:593–600.

Oesterhelt, D. 1982. Reconstitution of the retinal proteins bacteriorhodopsin and halorhodopsin. *Methods Enzymol.* 88:10–17.

Onishi, H., M. E. McCance, and N. E. Gibbons. 1965. A synthetic medium for extremely halophilic bacteria. *Cand. J. Microbiol.*11:365–373.

Perrin, F. 1934. Movement Brownien d'un ellipsoide (I). Dispersion diélectrique pour des molécules ellipsoidales. *J. Phys. Radium* 5:497–511.

Stoeckenius, W., R. H. Lozier, and R. A. Bogomolni. 1979. Bacteriorhodopsin and purple membrane of halobacteria. *Biochim. Biophys. Acta.* 505:215–278.

Stoeckenius, W., and R. A. Bogomolni. 1982. Bacteriorhodopsin and related pigments of halobacteria. *Annu. Rev. Biochem.* 51:587–615.

Sumper, M., H. Reitmeier, and D. Oesterhelt. 1976. Biosynthesis of the purple membrane of halobacteria. *Angew. Chem. Int. Ed. Engl.* 15:187.

Tristram-Nagle, S., C. P. Yang, and J. F. Nagle. 1985. Thermodynamic measurements of purple membrane. *Biophys. J.* 47(2, Pt. 2):93*a*. (Abstr.)